



Traffic Modeling and Analysis in the Performance of Parking Sensor Networks

Trista Lin, Hervé Rivano, Frédéric Le Mouél

**RESEARCH
REPORT**

N° 8480

December 2013

Project-Team URBANET



Traffic Modeling and Analysis in the Performance of Parking Sensor Networks

Trista Lin*, Hervé Rivano*, Frédéric Le Mouél†

Project-Team URBANET

Research Report n° 8480 — December 2013 — 21 pages

Abstract: Network traffic model is a critical problem for urban application, mainly because of its diversity and node density. As wireless sensor network is highly concerned with the development of smart cities, careful consideration to traffic model helps choose appropriate protocols and adapt network parameters to reach best performances on energy-latency tradeoffs. In this paper, we compare the performance of two off-the-shelf medium access control protocols on two different kinds of traffic models, and then evaluate their application-end information delay and energy consumption while varying traffic parameters and node density. From the simulation results, we highlight some limits induced by node density, occurrence frequency and non-uniform characters of event-driven applications. When it comes to real-time urban services, a protocol selection shall really be taken into account - even dynamically - with a special attention to energy-delay tradeoff. To this end, we provide several insights on parking sensor networks.

Key-words: parking sensor network, network traffic modeling, information delay

* INRIA, Université de Lyon, INSA-Lyon, CITI-INRIA, F-69621, Villeurbanne, France

† Shanghai JiaoTong University, No.800 DongChuan Rd., Shanghai, China

**RESEARCH CENTRE
GRENOBLE – RHÔNE-ALPES**

Inovallée
655 avenue de l'Europe Montbonnot
38334 Saint Ismier Cedex

Modélisation du trafic et analyse de la performance des réseaux de capteurs de stationnement

Résumé : Les réseaux de capteurs sans fil sont essentiels au développement des villes intelligentes. Pour les étudier, les modèles de trafic employés sont cruciaux pour prendre en compte les spécificités des applications urbaines, ainsi que la diversité et la densité des noeuds. Dans ce travail, nous comparons les performances de deux protocoles classiques de contrôle d'accès au médium (MAC) sur deux modèles de trafic différents. Nous nous intéressons à leur performances en termes d'efficacité énergétique et de délai d'acheminement de l'information en fonction de l'intensité de l'activité mesurée et de la densité du réseau. Nous mettons en évidence les limites de pertinence de chaque approche et en dérivons des conseils sur les paramètres à utiliser en fonction de la situation ainsi que des perspectives vers des protocoles s'adaptant aux conditions réelles de l'activité mesurée.

Mots-clés : réseau de capteurs de stationnement, la modélisation du trafic de réseau, délai des informations

1 Introduction

As the urban population is increasing it brings the economic growth and the denser urban mobility[22]. The first to be affected is the traffic. Thanks to the smartphone technology, drivers can get diverse urban information simply from mobile app or internet. Thus, the availability and quality of urban information become the most important criteria for cities. Two general types of information are real-time and non real-time. The former is time-sensitive and tells current status or upcoming events, for example, traffic, public transit, surveillance and so on. The latter is time-insensitive and tells the timeless information, history, forecast or schedule, for example, environmental monitoring, weather forecast, local travel information and so on. The content of information can be generated and maintained by government institutions, firms, users or wireless networked sensors. User-generated content is crowdsourced data which enriches the information sources at different prospects. Plenty of interesting information can also be shared according to users' sudden or periodic urban mobility. The published content could, however, be outdated or false because of insufficient participants or malicious users, as well as limited to human's observation. In view of this fact, wireless networked sensors help obtain more various types of information and assure of the accurate measurement. According to information types, sensors send updated information periodically, on demand or burstingly. That is, a network packet which consists of certain information, shall be treated with its corresponding priority so as to respect an acceptable information delay[26]. Here, we are interested in the possible services which can be carried out by networked sensors due to the increasing mobility need. Among which, the traffic congestion is the greater thought at present and a huge percent of traffic jams are caused by the vehicles looking for parking spaces. So far as urban drivers are concerned, smart on-street parking system assisted by networked sensors is needed to shorten the parking search time and the parking distance from destinations.

Parking sensor network is formed by different types of networked sensors, which can detect vehicle's presence. Sensors which collect data 24 hours a day, allow us to follow up the congestion problem anytime. Two categories of sensing methods are stationary and mobile. Stationary sensors normally fixed on the pavement, curb, parking meter, or above parking spaces can detect parking occupancy within the sensing range. Mobile sensors mounted on vehicles can do likewise in movement, accordingly the detection range is larger yet much less reactive. For this reason, municipalities tends to install thousands of on-site parking sensors in the city centre, and, our studies also focus on this type of sensor networks.

Parking sensor networks as the general urban sensor network has the following problems to tackle:

Link quality Parking sensors are installed along the curb so that the wireless signal is easily affected by the changing urban environment. By now, link quality is normally assessed by several indicators in a field test. In view of stochastically varying link status, periodic traffic model is often applied in urban application to inform gateways of sensors' existences.

Node density Sensor deployment affects the medium access method and network load. Owing to the lack of multiple detection, parking sensors are merely gotten done in demarcated spaces, to wit, one vehicle detection sensor per space. By assuming that N parking sensors are served by one gateway, the distance between any two parking sensors s_i and s_j where $1 \leq i, j \leq N$ will satisfy $\|s_i - s_j\| \geq l$ whenever $i \neq j$. However, the communication range of each gateway is bounded so that N will not be arbitrarily large.

Traffic variation The design of network protocols shall be tailor-made for the need of networked sensors which is application-oriented and can be described by traffic models. If the selected application demands a real-time service from the network, protocols must be reactive enough to respect the minimum latency. In smart parking application, the information delay is quite strict. Three mainstream traffic models are request, event and time-driven. Request-driven is irrelevant for smart parking application since continuous recording is required. Time-driven application which generates periodic traffic is often used in testing the performance of network protocols because of its weak dependence on the environment. Event-driven application is knotty due to its variety on different types of observed events.

Our network structure comprises three components: parking sensor, gateway and mobile vehicle. Parking sensor is the measurement point, to wit the source of information, and stationary just like the parking space it is watching. Gateway plays two roles which are to aggregate the information from parking sensors and disseminate the aggregated information to vehicles according to their respective interests. Mobile vehicle is the network participant with an interest of parking spaces in the vicinity of a given destination. To carry out a smart parking service, diverse application models between the three components shall be discussed in order to design adapted network protocols. In this report, the application models between parking sensors and gateways are studied because the deployment of sensor nodes and the design of network will be critical for the subsequent information dissemination. Our body of work is to simulate the traffic influence on stationary WSN with the aim of ameliorating the design of network architecture in order to achieve its best performance in an urban environment and reduce the urban traffic. The problem we are addressing is the impact of urban parking density, event frequency and non-uniform traffic parameters to the real-time service constraints. We verified the impact of traffic variation on event and time driven applications through fixed and dynamic bandwidth allocations or through different number of sensors. Our contributions are summarized as follows:

1. Modeling of event- and time-driven urban smart parking applications by observing vehicle's arrival and departure.
2. Energy and delay performance evaluation of event- and time-driven applications through extensive experiments on urban scenarios, helps to find out the network limit with traffic variation in two typical bandwidth allocation protocols.
3. Engineering insights to streamline the WSN construction of urban smart parking applications, help network designers select applicable protocols and optimize the network performance.

2 Background and related works

Smart on-street parking application has received a lot of attention in recent years. Its main missions are to collect the real-time parking occupancy information and to disseminate these information to drivers simply through smart parking app. Two types of collection methods are mobile and stationary. The former is to take advantage of vehicle's mobility to collect information along the route. In which, the most economical is crowd-based mobile application. But the crowdsourced information is frequently unavailable, outdated or false because of insufficient participants, freeriders and malicious users[6, 2, 10, 13]. Therefore, it is obvious that crowdsourcing parking assistance system can not really provide a reliable real-time time service required by municipalities[19]. Alternatively, an ultrasonic sensor can be side-mounted on a taxicab or bus so as to detect an on-street parking spot map. For example, the ParkNet system in San

Francisco[17], collects data with the location information from GPS receiver and then transmit it over a cellular uplink every 60 seconds to the central server. Such a mobile parking sensor system requires much less installation, yet needs a longer average inter-polling time, to wit, 25 minutes for 80% of the cells in busier downtown area with only 300 cabs. Stationary collection method is to install on-site vehicle detection sensors[20] so as to monitor the occupancy status of parking spaces. Based on this, large-scale road-side parking sensor network has been implemented in many cities.

SFpark project[23] is the earliest municipal smart parking project which adopted 8200 stationary in-ground parking sensors and deployed a large-scale of multi-hop parking sensor networks in the downtown area of San Francisco. Each parking sensor, in communication with nearby relays, records when vehicles come and leave. The information delay is calculated by how long it takes the sensor network to process and sends out a event. 85% of events can be received within 60 seconds. Each sensor sends a message everyday even if the occupancy status doesn't change. Also SFpark applies a dynamic pricing policy in order to keep a 75% occupancy rate in any parking blocks. LA Express park[14] adopts a multi-hop parking sensor network in Los Angeles. In addition, the communication module uses Dust Networks' TSMP protocol [18, 24], designed to operate on multiple channels. Physically the wireless channel is divided up in time and frequency, and each resulting unit of the channel is assigned to satisfy data flow requirements, mainly event-driven. Similarly, Fastprk[8] project also installed stationary in-ground parking sensors in Barcelona and follows the Zigbee certification. Parking sensors send a message when the occupancy status changes and every 20 minutes to inform the gateway their existences. Nice park is one application of Connected Boulevard project in Nice. Parking sensors send a message with update information every 60 seconds or while the occupancy status changes. Thus the parking system is updated every 10 seconds and drivers pays their parking fee by second. Each sensor can work up to 8 years. Beijing city also implemented a smart parking system. Parking sensors detect the vehicle's presence every 8 seconds and then transmit the information to the central server. The in-ground parking sensor can work for 5 years without replacing battery. The disadvantage of in-ground parking sensors is the installation and the lack of multiple detection, nor the dimension of parked vehicle. That is, only demarcated parking area is supported. Conversely ParkNet can work on the detection of demarcated and un-demarcated parking area if the parking map is known in advanced.

Parking sensor network is a specialized form of WSN and certainly inherits its problems, viz energy-efficiency, latency and throughput. These indicators are all related to the design of network protocols[3, 29, 11, 1, 15, 21]. The tasks of parking sensor networks are to get real-time information of parking space availability and to have good resilience to adapt the traffic variation. Thus, the latency takes an utmost important role among all the factors. To optimize network parameters for the best performance of sensor networks, the network traffic and phenomenon are relevant. The measurement of vehicle arrival and departure, the key factor of generating network traffic, is one body two sides, either vehicles equipped with GPS receiver know their own locations for mobile detection, or install external on-site sensors for stationary detection. Vehicle arrival and departure have been studied in several kinds of real-time urban events, for example, public transit vehicle real-time position, traffic signal control according traffic flow and some closed car parks[12, 30, 28]. As previously mentioned, among three types of traffic models, request-driven does not fix the need of municipalities nor the quality of service[16] required for real-time application. Hence, a caching platform is preferred to build on the gateway so as to store the current parking occupancy information and response rapidly to parking queries from nearby drivers[5]. Also, it helps reduce the system delay time if applying centralized or decentralized dynamic parking resource allocation[9]. Since the arrival and departure are assumed Poisson distributed, the occupancy rate of the parking system can be analyzed by Markov process[4].

3 Network traffic model

The underlying parameters for simulating the network traffic are start time, duration, interval, packet size and the procedure. In urban sensor network, sensors are often stationary to monitor certain events, and thence the packet transmission shall always happen and never end. In other words, the key point of modeling an event-driven application will be to find an appropriate distribution to define the traffic interval, viz inter-event interval. Next, we present the modeling of the event occurrence and the definition of information delay with respect to urban smart parking applications.

3.1 Vehicle's arrival and departure

In parking sensor networks, the main observed events are vehicles' arrivals and departures. Also, each vehicle arrival accompanies exact one departure prior to next arrival. To model it, we first look at the event occurrence sequence on one parking sensor. We suppose each parking sensor is precise enough and provides merely two status, namely occupied and vacant (figure 1). The interval from vehicle's arrival to departure is so-called occupancy time $T_{p,i}$ during which sensor i detects vehicle's presence. Likewise, the interval from one's departure to next arrival is vacant time $T_{v,i}$ during which sensor i detects nothing. Both $T_{p,i}$ and $T_{v,i}$ proper shall be described by a fitting distribution in order to approximate their randomness. By assuming that $T_{p,i}$ and $T_{v,i}$ are both exponentially distributed with rate parameters λ_i and μ_i , we have:

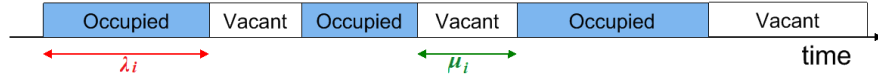


Figure 1: Occupancy status of one parking sensor over time

- The probability of choosing a occupancy time X can be calculated by $Pr(T_{p,i} = X) = \lambda_i e^{-\lambda_i X}$ and the mean is $E[T_{p,i}] = \lambda_i^{-1}$.
- The probability of choosing a vacant time Y can be calculated by $Pr(T_{v,i} = Y) = \mu_i e^{-\mu_i Y}$ and the mean is $E[T_{v,i}] = \mu_i^{-1}$.

After applying the exponential distribution, the timeline of sensor i 's parking status is shown in figure 2. The occupied period presents $T_{p,i}$ and the rest $T_{v,i}$. The average interval of vehicle's arrival will be $T_{p,i} + T_{v,i}$ and the average occupancy rate will be $T_{p,i}/(T_{p,i} + T_{v,i}) = \lambda_i^{-1}/(\lambda_i^{-1} + \mu_i^{-1})$. If $\lambda_i^{-1} > \mu_i^{-1}$, the average occupancy rate will be greater than 50%. Exponential distribution is one shape of Weibull so that the traffic interval can also be reshaped if needed. Besides, bursty traffic considered part of event-driven with Pareto distribution[25] is not discussed in our studies as one event can only be detected by one parking sensor at a time. In a business area, the parking status varies fast because of the parking time limit (λ_i is small) and the higher hot spot parking demand (μ_i is small).

Suppose that N networked parking sensors are installed in a district and form one subnet. These parking sensors can be installed along a street or in a crossroads. Each parking space i has average occupied and vacant periods λ_i^{-1} and μ_i^{-1} . Thus, the new parameters for global occupied and vacant time will be $\lambda = \sum_{i=1}^N \lambda_i$ and $\mu = \sum_{i=1}^N \mu_i$ such that the global parking occupancy rate will be $\lambda^{-1}/(\lambda^{-1} + \mu^{-1})$. In figure 3, it shows the time-varying occupancy rate's timeline of 24 parking sensors in a day while $\lambda = \mu$.

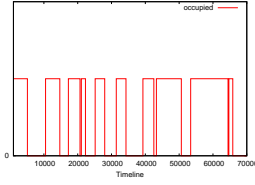


Figure 2: Sensor's occupancy status

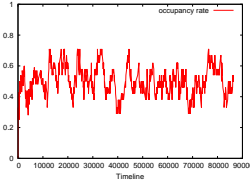


Figure 3: Occupancy rate in a district

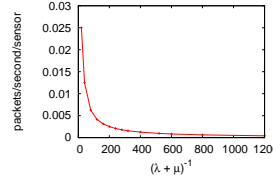


Figure 4: Generated packets by event-driven traffic model

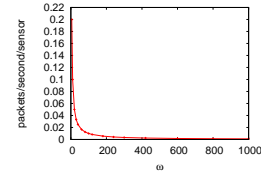


Figure 5: Generated packets by periodic traffic model

3.2 Event-driven traffic

The event occurrence frequency has a great impact on event-driven applications. Since each sensor node sends a packet while one vehicle arrives and another when it leaves, assume vehicle arrivals and departures are Poisson distributed with an average arrival and departure rates of α and β vehicles per second. Thus, the generated traffic will be $\alpha + \beta$ per second. For one parking space ($N = 1$), the relation between $(\alpha + \beta)$ and $(\lambda + \mu)^{-1}$ is shown in figure 4. In which, it is obvious that the product of $(\alpha + \beta)$ and $(\lambda + \mu)^{-1}$ is a constant.

$$(\alpha + \beta)(\lambda + \mu)^{-1} = k \quad (1)$$

Since there are N limited parking spaces, it means that the number of parked vehicles n_p in this area is between 0 and N . Assume the queueing model in this network with N parking sensors can be described by the birth and death process, one case of continuous-time Markov process, with a M/M/1/K queue, i.e., infinite input and output, 1 system and buffer size K. The probability of j parked vehicles is defined as $P_j(t)$. When a birth happens, the number of parked vehicles increases 1 with a birth rate α_j from state j to $j + 1$ where $\alpha_j = \alpha$ for $0 \leq j < N$. When a death happens, the number of parked vehicles decreases 1 with a death rate β_j from state j to $j - 1$ where $\beta_j = \beta$ for $0 < j \leq N$. The probability of zero parked vehicle $P_0(t)$ can only be reached by the transition from state one to zero so that $\alpha P_0(t) = \beta P_1(t)$. Similarly, the probability of i parked vehicles $P_i(t)$ in this area can be reached by the transition from the states $i - 1$ and $i + 1$ to i so that $\alpha P_i(t) = \beta P_{i+1}(t)$ and $(\alpha + \beta)P_i(t) = \alpha P_{i-1}(t) + \beta P_{i+1}(t)$. Let ρ equals to $\frac{\alpha}{\beta}$ where $\beta > \alpha$, then $P_i(t) = \rho P_{i-1}(t) = \rho^i P_0(t)$ where $P_0(t) = \frac{1-\rho}{1-\rho^{N+1}}$. The average number of parked vehicles n_p in this area can be calculated by equations 2 and 3.

The number of total parking spaces multiplied by the occupancy rate is the average number of parked vehicles:

$$n_p = N * \frac{\lambda^{-1}}{\lambda^{-1} + \mu^{-1}} \quad (2)$$

The expectation value of average parked vehicles stands for the average number of parked vehicles:

$$n_p = \sum_{k=0}^N k P_k(t) = \sum_{k=0}^N k \rho^k P_0(t) = \frac{1}{1-\rho} - \frac{1 + N\rho^{N+1}}{1-\rho^{N+1}} \quad (3)$$

According to Little's formula, the average number of parked vehicles n_p is equal to the product of vehicle arrival rate α and average parking time of N vehicles λ^{-1} , i.e., $n_p = \alpha \lambda^{-1}$. Hence, λ and μ can be calculated from the given α and β by equations 4 and 5, and vice versa.

$$\lambda^{-1} = \frac{n_p}{\alpha} = \frac{1}{\alpha} \left(\frac{1}{1-\rho} - \frac{1 + N\rho^{N+1}}{1-\rho^{N+1}} \right) = \frac{1}{\alpha} \left(\frac{\beta}{\beta - \alpha} - \frac{\beta^{N+1} + N\alpha^{N+1}}{\beta^{N+1} - \alpha^{N+1}} \right) \quad (4)$$

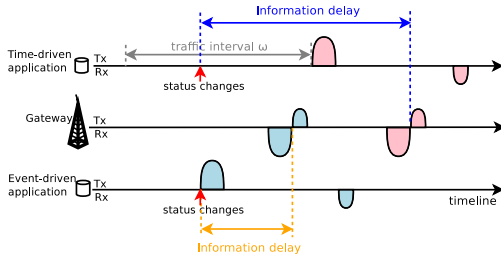


Figure 6: The calculation of information delay for event- and time-driven applications

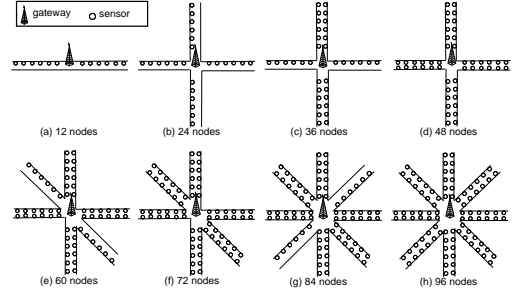


Figure 7: Topologies of different numbers of sensors. Increase the node density by adding one more line or one more side of curb parking.

$$\mu^{-1} = N\alpha^{-1} - \lambda^{-1} \quad (5)$$

Here λ and μ only stand for the global parameters of all the parked vehicles in the system. If we suppose all the parking spaces are uniform, each parking space has the same $\lambda_i = \frac{\lambda}{N}$ and $\mu_i = \frac{\mu}{N}$ for $1 \leq i \leq N$. But in real life, each parking space has different preferences according to their relative positions or commercial interests, for example, sensors have respective average parking and idle time according to the local commercial activities. That is to say, for any given λ and μ , the individual parameters λ_i and μ_i of each parking space can not be obtained. But these parameters will affect the performance according the protocols' properties.

3.3 Periodic/Time-driven traffic

On the contrary, time-driven application is only affected by the traffic interval ω instead of occurrence frequency. The amount of generated packets is inversely proportional to the traffic interval ω , shown in figure 5. While using periodic traffic model, the amount of network traffic is unaffected by the sensory information. It simply sends out a packet with the current time-stamped status when the time is up.

3.4 Definition of information delay

The main goal of parking sensor networks is to provide a real-time urban service to drivers. The principal performance indicator which we look at, therefore, is the *information delay*, defined as *the required time for knowing a changed occupancy status of a parking sensor*. Information delay is the sum of sensing duty-cycle, application delay, end-to-end delay and queuing delay. We have neglected the sensing duty cycle which is normally quite short. In event-driven application, each sensor sends out an updated information at once when detecting any event, namely, application delay is almost zero. Time-driven application is subject to the traffic interval so that an application delay shall be added up. In figure 6, we see that a longer traffic interval decreases the traffic intensity but also causes a longer information delay which is not preferable for real-time parking services.

Table 1: Simulation parameters

Transmit power output 3 dBm		Receive sensitivity -110 dBm		Data rate 250 kbps
P_{tx} 65.7 mW	P_{rx} 56.5 mW	P_{cs} 55.8 mW	P_{off} 30 μ W	$E_{radio.switch}$ 0.16425mJ
Transmission range 50m		Simulation time: 86400 seconds		Sensor node number: 12 - 96
Application parameters: Event-driven - λ & μ , Time-driven - ω				Packet size 84 bytes
MAC: duty-cycled fixed & dynamic bandwidth allocation, slot duration = 0.1s, retransmission and piggyback enabled.				

4 Urban smart parking application experiments with real-time service constraints

Bandwidth allocation can be fixed or dynamic. In this work we evaluate two off-the-shelf medium access control protocols: duty-cycled TDMA for fixed bandwidth allocation and duty-cycled CSMA for dynamic one. Our simulations, performed with the WSN simulator[27], use the topologies depicted in figure 7 with various node density. We evaluate the required energy consumption and the information delay of our traffic models in different scenarios. The distance between two adjacent sensors on the same road-side is 5 meters. The sensors in the vicinity of gateway are 10 meters away. That is to say, $\|s_i - s_j\| \geq l = 5$ whenever $i \neq j$.

Some simulation parameters are indicated in table 1, in which, each parking sensor can reach the gateway through one hop. Two types of bandwidth allocations are used to evaluate the impact of event-driven model compared with time-driven one. We choose to use off-the-shelf medium access control protocols, so that we can keep the objectivity in our simulation result and analysis without any exception of a particular protocol. Duty-cycled TDMA is used for fixed bandwidth allocation, and duty-cycled CSMA for dynamic bandwidth allocation¹.

4.1 Impact of node density

4.1.1 Fixed bandwidth allocation

Considering the sensor network is often bandwidth-limited, in single channel scenario, the only medium resource is time division. Each node is pre-assigned to one partition of medium resource in order to transmit their packets. While the network coordinator does not know in advance the traffic model and geolocation of each node, it pre-assigns an equal partition to nodes in the subnet. If a node has no packets to send in its term, the others still can not seize this occasion to send their packets.



Figure 8: Duty cycle of fixed bandwidth allocation

The duty cycle comprises an inactive period and $N + 1$ time slots for N parking sensors and gateway, shown in figure 8. Each sensor can only send its packet on its pre-assigned time slot. By assuming the inactive period = 0, the maximum capacity will be the reciprocal of slot duration s_i , viz 10 packets per second, and the duration of duty cycle can be calculated by $T_{duty.cycle} =$

¹Three points are not considered in our simulations that are the energy consumption of first synchronization, hourly changing traffic parameters, and the time-varying network throughput caused by the unstable link quality. Thus, all the retransmissions come merely of packet collision. The hourly changing traffic parameters λ_i and μ_i can be obtained from the existing municipal parking payment information.

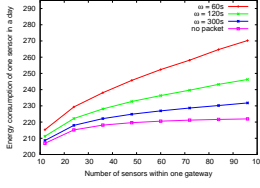


Figure 9: Per-node energy consumption of time-driven application under fixed bandwidth allocation

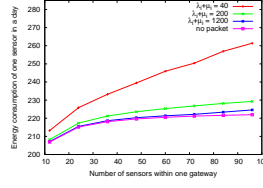


Figure 10: Per-node energy consumption of event-driven application under fixed bandwidth allocation

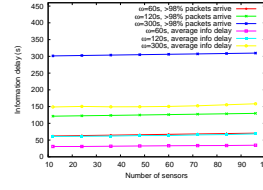


Figure 11: Information delay of time-driven application while N and traffic parameters change under fixed bandwidth allocation

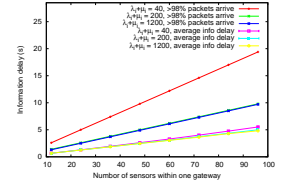


Figure 12: Information delay of event-driven application while N and traffic parameters change under fixed bandwidth allocation

$(N + 1) * s_i = 0.1(N + 1)$. If the packet transmission is failed on the current time slot, the next one will be in $0.1(N + 1)$ seconds. To minimize the idle listening period, each transmitter sends a very small reservation beacon message before starting the data transmission. If the reservation fails (the receiver is unreachable), the transmitter will put the packet into the queue, turn off its radio and wait for the next time slot. Instead of wasting energy to do a vain transmission, sensor nodes prefer to evaluate the receiver's availability through these very small beacons. The advantages of fixed bandwidth allocation are the much less packet collision and lower energy consumption since nodes only send beacons in certain slots. If sensor nodes' traffic model is given and static, fixed bandwidth allocation can optimize the resource assignment in order to reach a better performance. The drawbacks are that many time slots are wasted so that a longer delay time is caused, also the urban traffic model is dynamic and time-variant. Since each node included the gateway has its corresponding time slot, that is, the gateway needs to know the amount of nodes in its subnet in order to allocate the resource. If there is a new node which intends to join this network, the gateway will have to reallocate the resource while there is no enough time slots.

Figures 9 and 10 shows the per-node energy consumption using time- and event-driven network traffic while the number of sensors varies. It is obvious that the per-node energy consumption is elevated while the node density increases, even increasingly significant when the traffic intensity is high ($(\lambda + \mu)^{-1}$ or ω is small). If the traffic intensity is not that high, the energy consumption is elevated in the beginning on grounds of additional control packets and then stabilized. But when it comes to information delay, the situation is not the same. Figure 11 shows the information delay of time-driven model is merely ω -related. Figure 12 shows that the information is proportional to the number of sensors because of the duty cycle amplified with the number of nodes N .

4.1.2 Dynamic bandwidth allocation

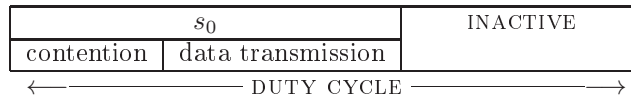


Figure 13: Duty cycle of dynamic bandwidth allocation

Dynamic bandwidth allocation uses contention-based medium access control due to the flexible resource allocation previously mentioned. The principle is that the node gets its partition of

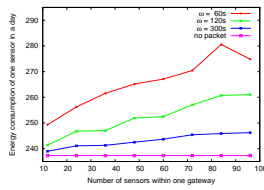


Figure 14: Per-node energy consumption of time-driven application under dynamic bandwidth allocation

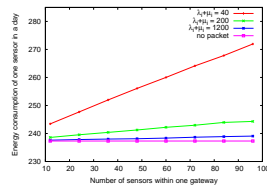


Figure 15: Per-node energy consumption of event-driven application under dynamic bandwidth allocation

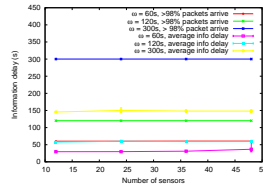


Figure 16: Information delay of time-driven application while N and traffic parameters change under dynamic bandwidth allocation

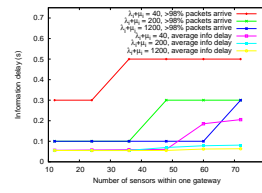


Figure 17: Information delay of event-driven application while N and traffic parameters change under dynamic bandwidth allocation

network resource when it asks for. If more than two nodes declare their demands, a competition will be held to choose who is the current transmitter. Nodes who lose the competition will go to sleep and wait for next resource allocation. If the competition method is not good enough, the packet collision will happen frequently and drop the network performance. To do that, nodes listen to the channel to know if the channel is busy before sending a packet. If the channel is busy, nodes will put the packet into their queues and wait for next competition. Otherwise, nodes will send out a beacon message with the reservation information. If the desired receiver gets this packet, it will reply an acknowledgment and then a transmission reservation is done. Also considering the bandwidth is limited, the network resource is also time-division.

So as to reduce the idle listening, a duty cycle is also applied and contains the contention, data transmission and inactive periods, shown in figure 13. The advantages of dynamic resource allocation are the better use of network resource and a short network delay. The drawbacks is the inevitable packet collision which causes arbitrarily high energy consumption and latency on grounds of endless contentions triggered by high node density. By assuming the inactive period is equal to zero and the slot duration is 0.1 seconds, the maximum capacity will be the reciprocal of slot duration, viz 10 packets per second and the duration of duty cycle is 0.1 seconds. If there is a new node which intends to join this network, it will just join the competition and increase the packet collision rate.

Figure 14 and 15 show the per-node energy consumption of time- and event-driven models while N varies. Unlike the previous case, the elevated energy consumption is mainly provoked by the increasing competitors during each contention period. While $\omega = 60s$ and $N = 96$, the energy consumption declines, inasmuch as excessive packet collisions cause no successful transmission reservation. Figure 16 shows the information delay of time-driven model which is ω -related as well. After N is greater than 60, the information delay is also arbitrarily large due to the very high packet collision rate. However, in event-driven model, the information delay is also proportional to the duty cycle. The difference is that the duty cycle of dynamic bandwidth allocation does not vary with N , thus each node tries to send its packets within κ times of duty cycle where κ is a constant. The more transmission demands, the greater value of κ , shown in figure 17. Even the average information delay is just a little bit higher than the half of duty cycle, the global information delay can still vary to 5 times of duty cycle. Hence, 0.5 seconds is considered as the guaranteed maximum information delay.

4.2 Impact of traffic intensity

The simulation we ran in this section used the topology in figure 7(b) with 24 nodes.

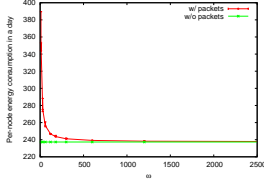


Figure 18: Per-node energy consumption of time-driven application under dynamic bandwidth allocation while $N = 24$

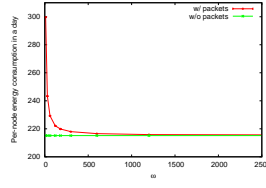


Figure 19: Per-node energy consumption of time-driven application under fixed bandwidth allocation while $N = 24$

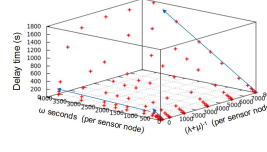


Figure 20: Information delay - dynamic bandwidth allocation - time-driven with varied λ , μ and ω

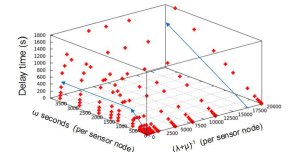


Figure 21: Information delay - fixed bandwidth allocation - time-driven with varied λ , μ and ω

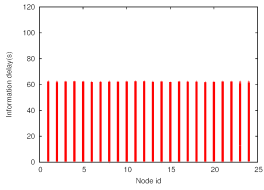


Figure 22: Information delay - Fixed bandwidth allocation - non-uniform - $(\lambda + \mu)^{-1} = 1.667 - \omega = 60s$

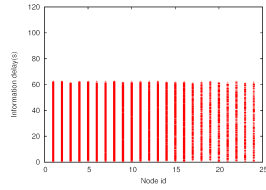


Figure 23: Information delay - Fixed bandwidth allocation - non-uniform - $(\lambda + \mu)^{-1} = 8.33 - \omega = 60s$

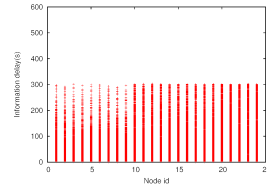


Figure 24: Information delay - Fixed bandwidth allocation - non-uniform - $(\lambda + \mu)^{-1} = 1.667 - \omega = 300s$

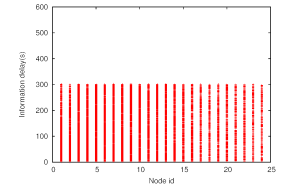


Figure 25: Information delay - Fixed bandwidth allocation - non-uniform - $(\lambda + \mu)^{-1} = 8.33 - \omega = 300s$

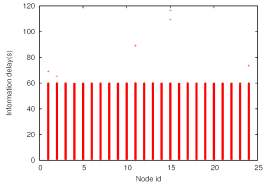


Figure 26: Information delay - Dynamic bandwidth allocation - non-uniform - $(\lambda + \mu)^{-1} = 1.667 - \omega = 60s$

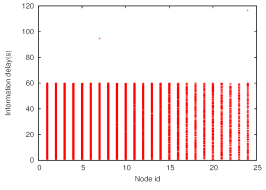


Figure 27: Information delay - Dynamic bandwidth allocation - non-uniform - $(\lambda + \mu)^{-1} = 8.33 - \omega = 60s$

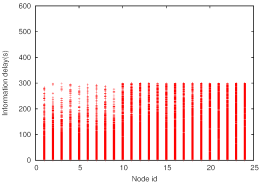


Figure 28: Information delay - Dynamic bandwidth allocation - non-uniform - $(\lambda + \mu)^{-1} = 1.667 - \omega = 300s$

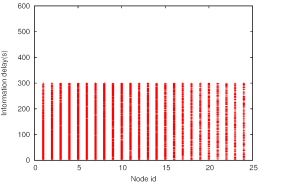


Figure 29: Information delay - Dynamic bandwidth allocation - non-uniform - $(\lambda + \mu)^{-1} = 8.33 - \omega = 300s$

4.2.1 Periodic/time-driven traffic parameter

Since periodic traffic is less affected by the bandwidth allocation method and strongly related to the traffic interval ω , figures 18 and 19 show the relation between traffic interval ω and per-node energy consumption. The periodic traffic is equivalent to constant bit rate so that the traffic is known and uniform among all sensor nodes. Hence the deviation of consumed energy is not apparent. However, it is obvious that the consumed energy is extremely low while $\omega \geq 1200$. In other words, the information delay which is proportional to 1200 will not be acceptable for real-time urban service. But it is interesting to assign a periodic traffic with a long interval on sensor nodes simply to inform gateways of their existences and current battery status. Figures 20 and 21 show the information delay in function and $(\lambda + \mu)^{-1}$ and ω . Note that in periodic/time-driven application, sensor verifies the occupancy status every ω second and then sends a packet with

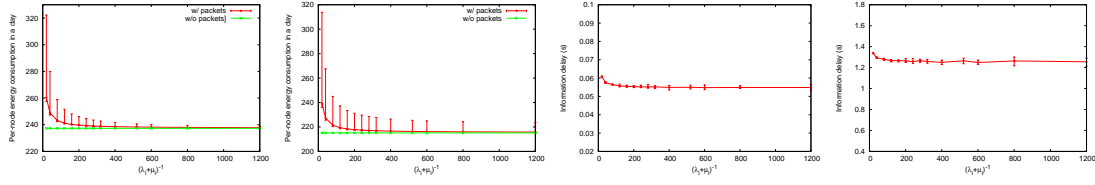


Figure 30: Per-node energy consumption of event-driven application under dynamic bandwidth allocation while $N = 24$

Figure 31: Per-node energy consumption of event-driven application under fixed bandwidth allocation while $N = 24$

Figure 32: Average information delay while the traffic parameters change and $N = 24$ under dynamic bandwidth allocation

Figure 33: Average information delay while the traffic parameters change and $N = 24$ under fixed bandwidth allocation

the sensed information to gateways. Thus, if sensor changes its occupancy more than two times in ω seconds, the updated information will not be recorded anywhere and the current status will also be less antique. When $(\lambda_i + \mu_i)^{-1} > \omega$, the information delay time is proportional to $\frac{\omega}{2}$, otherwise, $2(\lambda_i + \mu_i)^{-1}$. The bandwidth allocation methods make no difference to the information delay.

In figures 22 and 23, we see that when ω is 60 seconds, the variation of $(\lambda_i + \mu_i)^{-1}$ only affects the amount of packets, the maximum and average information, however, are not affected at all. Therefore, when ω is 300 seconds, $(\lambda_i + \mu_i)^{-1}$ does affect the average information. In figures 24 and 25, the effect of $(\lambda_i + \mu_i)^{-1}$ is obvious. The information delay of packets from nodes 1-9 is much shorter than the others. That is because their traffic parameters are more active than the period interval, namely $(\lambda_i + \mu_i)^{-1} \ll \omega$ for $1 \leq i \leq 9$. In addition, in figures 23 and 25, the packet number is reduced as the node id increases. Take dynamic bandwidth allocation to substitute the fixed one and see the results in figures 26-29. In this way, some updated information will be missed if the sensor does not store it into the buffer. As previously mentioned, neither bandwidth allocation method affects the performance of time-driven application.

4.2.2 Event-driven traffic parameters

Besides node density, the impact of traffic variation on energy consumption and information delay is also important. Figures 30 and 31 shows the per-node energy consumption when the traffic parameters vary under fixed and dynamic bandwidth allocations. Compared with figure 18 and 19, we see that the consumed energy deviation is caused by the traffic difference among sensor nodes, in particular in the fixed bandwidth allocation. That is because fixed bandwidth allocation is more susceptible to network traffic. Similarly, the average information delay in figures 32 and 33 also shows a higher deviation in fixed bandwidth allocation.

To explain this phenomenon, we compare the information delay with uniform and non-uniform parameters. In figure 34 and 35, $(\lambda + \mu)^{-1} = 1.667$. By assuming all the N parking spaces are uniform, $\lambda_i = \frac{\lambda}{N}$ and $\mu_i = \frac{\mu}{N}$ for $1 \leq i \leq N$. The uniform simulation result is shown in figure 34. If the N parking spaces are non-uniform, set $\lambda_i \leq \lambda_j$ and $\mu_i \leq \mu_j$ for $i \leq j$ such that $(\sum_{i=1}^N \lambda_i + \sum_{i=1}^N \mu_i)^{-1} = (\lambda + \mu)^{-1} = 1.667$. Then in figure 35, we see that some nodes which have a smaller $(\lambda_i + \mu_i)^{-1}$ have to transmit more packets but can not have more assigned time-slots so that a longer information delay is provoked.

On the contrary, apply the same traffic parameters in dynamic bandwidth allocation and compare the results in figures 36 and 37. It is obvious that the traffic variation does not affect the information latency in dynamic bandwidth allocation, as well as $(\lambda + \mu)^{-1} = 8.333$ in figure

38 and 39.

Even enlarge the value of $(\lambda + \mu)^{-1}$ to 50 with respective different λ_i and μ_i values, it can still be seen that node 1 and 2 in figure 40 have several packets with a longer information delay but not in figure 41. It means even the network resource is adequate for all generated packets, an inflexible allocation method can still collapse the network performance.

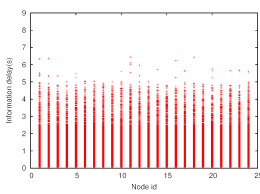


Figure 34: Information delay - fixed bandwidth allocation - uniform - $(\lambda + \mu)^{-1} = 1.667$

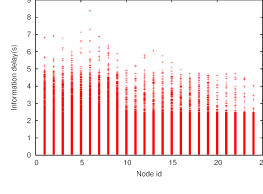


Figure 35: Information delay - fixed bandwidth allocation - non-uniform - $(\lambda + \mu)^{-1} = 1.667$

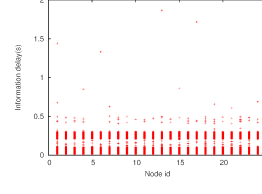


Figure 36: Information delay - dynamic bandwidth allocation - uniform - $(\lambda + \mu)^{-1} = 1.667$

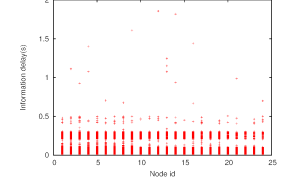


Figure 37: Information delay - dynamic bandwidth allocation - non-uniform - $(\lambda + \mu)^{-1} = 1.667$

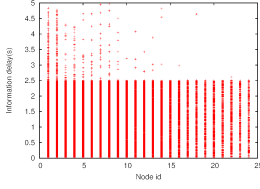


Figure 38: Information delay - fixed bandwidth allocation - non-uniform - $(\lambda + \mu)^{-1} = 8.333$

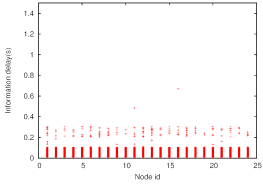


Figure 39: Information delay - dynamic bandwidth allocation - non-uniform - $(\lambda + \mu)^{-1} = 8.333$

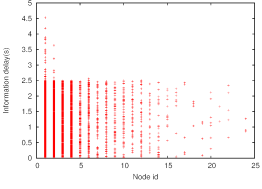


Figure 40: Information delay - fixed bandwidth allocation - non-uniform - $(\lambda + \mu)^{-1} = 50$

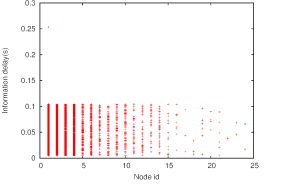


Figure 41: Information delay - dynamic bandwidth allocation - non-uniform - $(\lambda + \mu)^{-1} = 50$

4.3 Multiple hop

Table 2: Transmission power at 2 hops[7]

Transmit power output: 0 dBm	P_{TX} : 48 mW
------------------------------	------------------

The transmission range of sensor nodes is proportional to its transmit power output, as well as the power consumption per unit of time. While the transmission range is reduced, sensor node could be out of the communication range of the gateway and then could only send out its packets via its neighbors. The simulation results in figure 42-53 use a lower transmission power, shown in table 2. Here we first look at the fixed bandwidth allocation. In figures 42-44, we see that information delay for nodes, which are two hops far away, is increased by one more duty-cycle duration. But if the traffic parameters are non-uniform, the information delay can be amplified on certain nodes due to the inflexible bandwidth allocation, shown in figures 45-47. Also, if the further nodes and their relays (nodes 1-5) both have a lot of packets to send, the delay time will be even more severe.

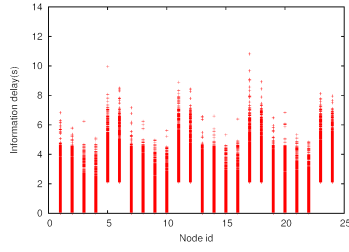


Figure 42: Information delay - Fixed bandwidth allocation - uniform - $(\lambda + \mu)^{-1} = 1.667 - 2$ hops

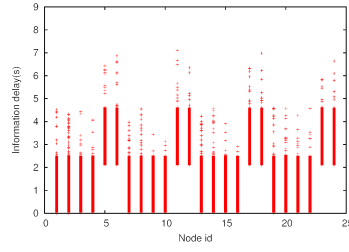


Figure 43: Information delay - Fixed bandwidth allocation - uniform - $(\lambda + \mu)^{-1} = 8.33 - 2$ hops

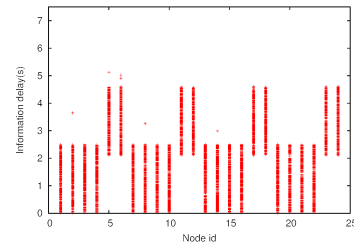


Figure 44: Information delay - Fixed bandwidth allocation - uniform - $(\lambda + \mu)^{-1} = 50 - 2$ hops

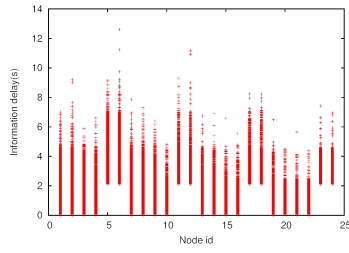


Figure 45: Information delay - Fixed bandwidth allocation - non-uniform - $(\lambda + \mu)^{-1} = 1.667 - 2$ hops - $(\lambda_i + \mu_i)^{-1} \leq (\lambda_j + \mu_j)^{-1}$ when $i \leq j$

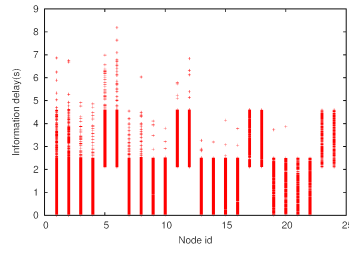


Figure 46: Information delay - Fixed bandwidth allocation - non-uniform - $(\lambda + \mu)^{-1} = 8.33 - 2$ hops - $(\lambda_i + \mu_i)^{-1} \leq (\lambda_j + \mu_j)^{-1}$ when $i \leq j$

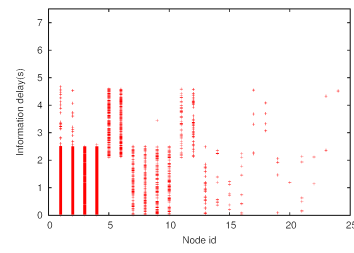


Figure 47: Information delay - Fixed bandwidth allocation - non-uniform - $(\lambda + \mu)^{-1} = 50 - 2$ hops - $(\lambda_i + \mu_i)^{-1} \leq (\lambda_j + \mu_j)^{-1}$ when $i \leq j$

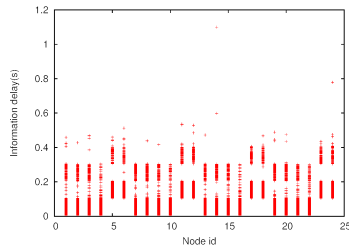


Figure 48: Information delay - Dynamic bandwidth allocation - uniform - $(\lambda + \mu)^{-1} = 1.667 - 2$ hops

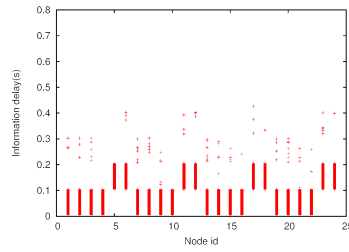


Figure 49: Information delay - Dynamic bandwidth allocation - uniform - $(\lambda + \mu)^{-1} = 8.33 - 2$ hops

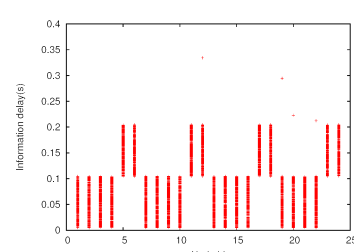


Figure 50: Information delay - Dynamic bandwidth allocation - uniform - $(\lambda + \mu)^{-1} = 50 - 2$ hops

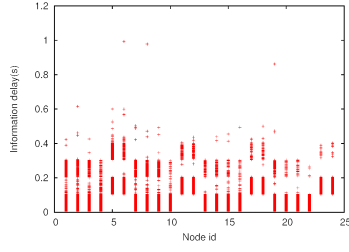


Figure 51: Information delay - Dynamic bandwidth allocation - non-uniform - $(\lambda + \mu)^{-1} = 1.667 - 2$ hops - $(\lambda_i + \mu_i)^{-1} \leq (\lambda_j + \mu_j)^{-1}$ when $i \leq j$

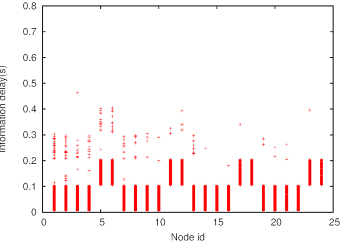


Figure 52: Information delay - Dynamic bandwidth allocation - non-uniform - $(\lambda + \mu)^{-1} = 8.33 - 2$ hops - $(\lambda_i + \mu_i)^{-1} \leq (\lambda_j + \mu_j)^{-1}$ when $i \leq j$

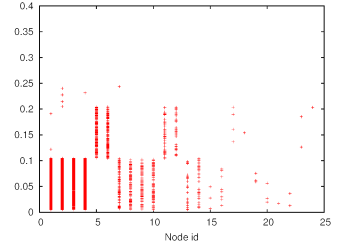


Figure 53: Information delay - Dynamic bandwidth allocation - non-uniform - $(\lambda + \mu)^{-1} = 50 - 2$ hops - $(\lambda_i + \mu_i)^{-1} \leq (\lambda_j + \mu_j)^{-1}$ when $i \leq j$

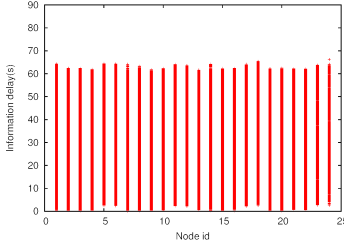


Figure 54: Information delay - Fixed/Dynamic bandwidth allocation - non-uniform - $(\lambda+\mu)^{-1} = 1.667$ - $\omega = 60s$ - 2 hops

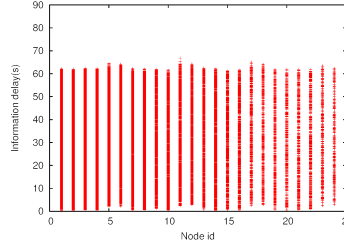


Figure 55: Information delay - Fixed/Dynamic bandwidth allocation - non-uniform - $(\lambda+\mu)^{-1} = 8.33$ - $\omega = 60s$ - 2 hops

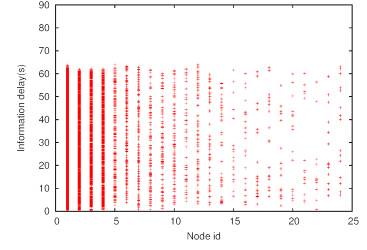


Figure 56: Information delay - Fixed/Dynamic bandwidth allocation - non-uniform - $(\lambda+\mu)^{-1} = 50$ - $\omega = 60s$ - 2 hops

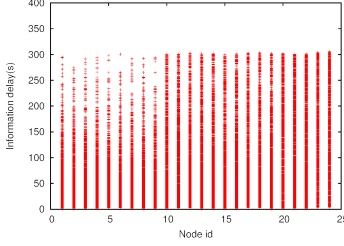


Figure 57: Information delay - Fixed/Dynamic bandwidth allocation - non-uniform - $(\lambda+\mu)^{-1} = 1.667$ - $\omega = 300s$ - 2 hops

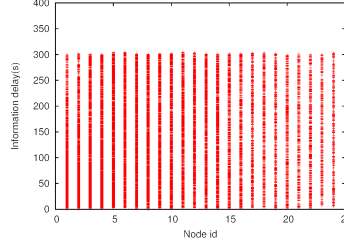


Figure 58: Information delay - Fixed/Dynamic bandwidth allocation - non-uniform - $(\lambda+\mu)^{-1} = 8.33$ - $\omega = 300s$ - 2 hops

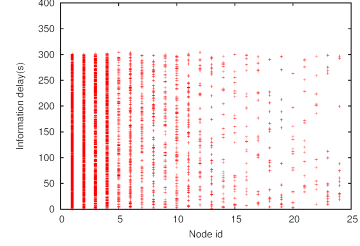


Figure 59: Information delay - Fixed/Dynamic bandwidth allocation - non-uniform - $(\lambda+\mu)^{-1} = 50$ - $\omega = 300s$ - 2 hops

Now we observe the same scenario in dynamic bandwidth allocation. In figures 48-50, these further nodes all have a longer information delay as well as in previous paragraph. While applying a non-uniform traffic parameters, the delay time in figures 51-53. In terms of fixed bandwidth allocation, dynamic bandwidth allocation adaptes much better to the variation of traffic parameters. But we can still see some packets from nodes 1-5 have a slightly longer delay which are caused by the competitive area and hidden terminal problem.

Multiple hop prolongs the information delay whichever application model is applied. In figures 54-56, as indicated in previous sessions, the maximum information is only related to the traffic interval ω plus one-hop delay, i.e., one time of duty-cycle duration. Only when the event occurrence frequency is high than the traffic interval, the average information delay will be shorter because of some losing data, in figure 57. As the traffic occurrence frequency reduces, the data loss is gradually unapparent, in figures 58 and 59. In addition, dynamic bandwidth allocation has more transmission conflict since multiple-hop network brings more hidden terminal in the network.

4.4 Duty cycle

From figures 8 and 13, we can see that duty cycle is mainly determined by slot duration which is, however, bounded by traffic model. The minimum slot duration s_{min} shall be long enough to complete a reservation and a piggybacked packet transmission so that packet size and data rate are the important factors. Nevertheless, the maximum slot duration s_{max} is limited by the minimum required throughput according to application. That is to say, if the slot duration is equal to s_i seconds, the maximum throughput will not exceed $\frac{1}{s_i}$ packets per second. Since

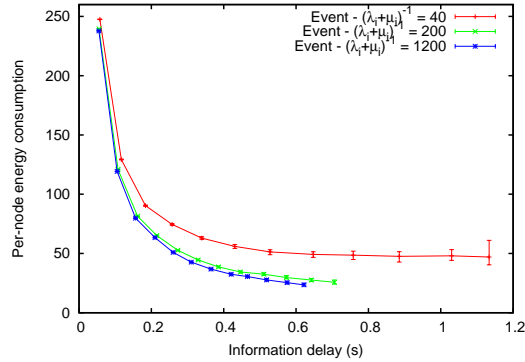


Figure 60: Per-node energy-delay tradeoff of event-driven application in dynamic bandwidth allocation while $N = 24$

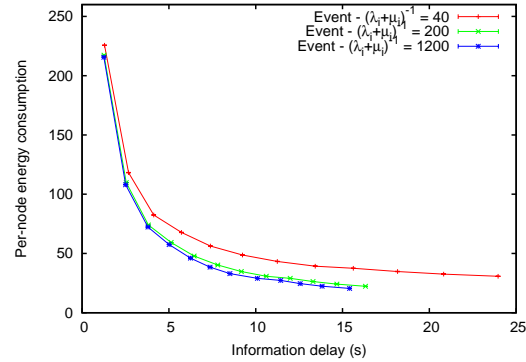


Figure 61: Per-node energy-delay tradeoff of event-driven application in fixed bandwidth allocation while $N = 24$

event-driven application is mainly proportional to the duty cycle, we varied slot duration from 0.1 to 1.2 seconds in the topology in figure 7(b) with 24 nodes and then got the energy-delay tradeoff.

Figure 60 shows the energy-delay tradeoff in dynamic bandwidth allocation. For $(\lambda_i + \mu_i)^{-1} = 40$, $s_{max,40} = 1.667$ and we can see that the energy deviation is more obvious when the slot duration approximates to $s_{max,40}$. Also the average information delay is equal to $\kappa * T_{duty.cycle} = \kappa s_i$ where κ varies from $\frac{1}{2}$ to approximately 1 when s_i increases. Figure 61 shows the energy-delay tradeoff in fixed bandwidth allocation. By replacing $T_{duty.cycle} = (N + 1)s_i$, the average information delay is equal to $\kappa(N + 1)s_i$ where κ varies from $\frac{1}{2}$ to approximately 1 when s_i increases. However, thanks to the extremely low collision rate in fixed bandwidth allocation, the energy deviation is still low even though we increase the slot duration.

Accordingly, while having the same slot duration, the energy consumption in dynamic bandwidth allocation is a bit higher, yet the information delay is much shorter. In other words, subject to the throughput conditions, for the same information delay, dynamic bandwidth allocation consumes significantly less energy than fixed one.

5 Engineering Insights

In this section, we summarize our results in section 4 and provide engineering insights to streamline the WSN construction of urban smart parking application. The bandwidth allocation method is the utmost important key point of determining energy consumption and information delay when traffic and node densities are known a priori. We applied two fundamental types of bandwidth allocations to our simulations instead of choosing particular protocols. In this way, we can see clearly that how the traffic and node densities affect the network performance and the results could serve as guidelines for urban sensor network designers. Since the network load is calculated by summing up the respective traffic load on each node, and shall not be greater than the network throughput, we discuss it separately from the following three viewpoints by referring to figure 62.

5.1 Node density

The network load elevates undoubtedly as the number of nodes N increases. In dynamic bandwidth allocation, the first to be affected is the rising packet collision rate because of more competitors in one time slot. When $N > 50$, the information delay becomes arbitrarily large. The energy consumption first rises due to the retransmission, and then falls, inasmuch as the channel is always busy. However, the contention method of dynamic bandwidth allocation can be improved to serve more sensor nodes, like what is done in [11, 1, 15]. Else, in fixed bandwidth allocation, the throughput is none the less on the downsides as N increases. This is due to the extension of duty cycle. That is to say, the network load of each node shall not be greater than the maximum network throughput, viz $\alpha_i + \beta_i \leq (T_{duty.cycle})^{-1} = (s_i * (N + 1) + T_{inactive})^{-1}$, to ensure the network is capable to process all the demands. Hence, Dynamic bandwidth allocation has a short information delay and is more adaptive to the non-uniform traffic parameters for $N \leq 50$, i.e, can be improved by a good contention method. Fixed bandwidth allocation can avoid the packet collision problem while the network density is high but still miss an optimal scheduling which considers routing and MAC protocols to improve its latency.

5.2 traffic intensity

The network load of node i is equal to $\alpha_i + \beta_i = k(\lambda_i + \mu_i)$. When the traffic intensity is high, event-driven application is suggested on grounds of its much shorter information delay. On the contrary, time-driven application generates excessive packets when ω is small, and the information delay is too long when ω is large. As previously mentioned, time-driven application is often used to inform gateway of sensors' existences, for example, to report the hourly battery status, also to provide the information of link quality. If $(\lambda_i + \mu_i)^{-1}$ is large enough, to wit event frequency is very low, the updated packet can be merged with other hourly information. In other words, in time-driven application, the energy consumption is extremely low for $\omega \gg 1200$. If $(\lambda_i + \mu_i)^{-1} \gg 2\omega$, and λ_i^{-1} and μ_i^{-1} are both much greater than 4ω , it means the event occurrence rate is low and time-driven can be considered. Another problem of time-driven application is their start time. If all sensor nodes have a very similar start time and traffic interval, a bursty traffic can be generated and gives an apparent influence on dynamic bandwidth allocation.

5.3 Duty cycle

What will happen if the network traffic and node densities are both high? When N is large, the throughput of fixed bandwidth allocation drops because of the extension of duty cycle. The maximum network throughput in fixed bandwidth allocation, calculated by the inverse of duty cycle $\frac{1}{(N+1)*s_i+T_{inactive}}$, shall be greater than $k(\lambda_i + \mu_i)$ or $\frac{1}{\omega}$ respectively in event- or time-driven applications. Because $k \approx 0.48$ and $(\lambda_i + \mu_i)^{-1} \gg 2\omega$ to apply time-driven application, we then get $k(\lambda_i + \mu_i) \ll \frac{1}{4\omega}$. Certainly $\frac{1}{\omega}$ exceeds $\frac{1}{(N+1)*s_i+T_{inactive}}$ faster than $\frac{1}{4\omega}$. By assuming N_m is the maximum number of nodes to apply time-driven application in fixed bandwidth allocation, we have $\frac{1}{(N+1)*s_i+T_{inactive}} = \frac{1}{\omega}$. Thus, $N_m = \frac{\omega}{s_i} - 1$ if $T_{inactive} = 0$.

6 Conclusion

In this report, we have studied parking sensor networks, especially focusing on delay constraints and energy efficiency issues from a viewpoint of traffic. Two types of traffic models, viz event- and time-driven, are performed with different rate parameters. We provide engineering insights for urban sensor network designers, in particular the best combination of traffic models and

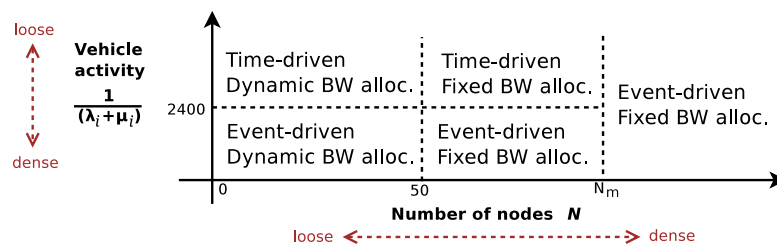


Figure 62: Best configuration versus vehicle activity and network density

bandwidth allocation depending on the urban activity and the node density. Even though these thresholds can be slightly shifted by particular optimized protocols, no doubt it retains a clear overview to build urban applications over WSNs. These insights highlight the importance to develop an adaptive MAC protocol which is able to distributedly detect the intensity of traffic and switch between event- and time-driven traffic model when required.

References

- [1] Abichar, Z., Chang, J.: Conti: Constant-time contention resolution for wlan access. In: NETWORKING 2005. Networking Technologies, Services, and Protocols; Performance of Computer and Communication Networks; Mobile and Wireless Communications Systems, Lecture Notes in Computer Science, vol. 3462, pp. 358–369. Springer Berlin Heidelberg (2005)
- [2] Ali, K., Al-Yaseen, D., Ejaz, A., Javed, T., Hassanein, H.: Crowdits: Crowdsourcing in intelligent transportation systems. In: 2012 IEEE Wireless Communications and Networking Conference (WCNC). pp. 3307–3311 (2012)
- [3] Anastasi, G., Conti, M., Francesco, M.D., Passarella, A.: Energy conservation in wireless sensor networks: A survey. *Ad Hoc Networks* 7(3), 537 – 568 (2009)
- [4] Andronov, A., Latkov, A., Revzina, J.: Internet traffic description on a base of markov-additive process of arrivals. In: 2011 Baltic Congress on Future Internet Communications (BCFIC Riga). pp. 212–217 (2011)
- [5] Caliskan, M., Graupner, D., Mauve, M.: Decentralized discovery of free parking places. In: Proceedings of the 3rd international workshop on Vehicular ad hoc networks. pp. 30–39. VANET '06, ACM, New York, NY, USA (2006)
- [6] Chen, X., Santos-Neto, E., Ripeanu, M.: Crowdsourcing for on-street smart parking. In: Proceedings of the second ACM international symposium on Design and analysis of intelligent vehicular networks and applications. pp. 1–8. DIVANet '12, ACM, New York, NY, USA (2012)
- [7] micaz datasheet, www.openautomation.net/uploads/productos/micaz_datasheet.pdf
- [8] Fastprk: Smart parking technology | smart city sensors, www.fastprk.com
- [9] Geng, Y., Cassandras, C.: A new smart parking system based on optimal resource allocation and reservations. In: 2011 14th International IEEE Conference on Intelligent Transportation Systems (ITSC). pp. 979–984 (2011)

- [10] Hoh, B., Yan, T., Ganesan, D., Tracton, K., Iwuchukwu, T., Lee, J.S.: Trucentive: A game-theoretic incentive platform for trustworthy mobile crowdsourcing parking services. In: 2012 15th International IEEE Conference on Intelligent Transportation Systems (ITSC). pp. 160–166 (2012)
- [11] Jamieson, K., Balakrishnan, H., Tay, Y.: Sift: a MAC Protocol for Event-Driven Wireless Sensor Networks. In: Third European Workshop on Wireless Sensor Networks (EWSN). Zurich, Switzerland (February 2006)
- [12] Jian Pan, Xiuting Dai, X.X., Lou, Y.: Public transit vehicle arrival information system based on mobile internet. *Applied Mechanics and Materials* 380-384 (August 2013)
- [13] Kokolaki, E., Kollias, G., Papadaki, M., Karaliopoulos, M., Stavrakakis, I.: Opportunistically-assisted parking search: A story of free riders, selfish liars and bona fide mules. In: 2013 10th Annual Conference on Wireless On-demand Network Systems and Services (WONS). pp. 17–24 (2013)
- [14] La express park: Save time, park smarter, www.laexpresspark.org
- [15] Lampin, Q., Barthel, D., Auge-Blum, I., Valois, F.: Cascading tournament mac: Low power, high capacity medium sharing for wireless sensor networks. In: Wireless Communications and Networking Conference (WCNC), 2012 IEEE. pp. 1544–1549 (2012)
- [16] Leone, R., Medagliani, P., Leguay, J.: Optimizing QoS in Wireless Sensors Networks using a Caching Platform. In: *Sensornets 2013*. p. 56. Barcelona, Spain (Feb 2013)
- [17] Mathur, S., Jin, T., Kasturirangan, N., Chandrasekaran, J., Xue, W., Gruteser, M., Trappe, W.: Parknet: drive-by sensing of road-side parking statistics. In: Proceedings of the 8th international conference on Mobile systems, applications, and services. pp. 123–136. MobiSys '10, ACM, New York, NY, USA (2010)
- [18] Pister, K.S.J., Doherty, L.: Tsmpt: Time synchronized mesh protocol. In: In Proceedings of the IASTED International Symposium on Distributed Sensor Networks (DSN08) (2008)
- [19] Polycarpou, E., Lambrinos, L., Protopapadakis, E.: Smart parking solutions for urban areas. In: 2013 IEEE 14th International Symposium and Workshops on a World of Wireless Mobile and Multimedia Networks (WoWMoM). pp. 1–6 (2013)
- [20] Revathi, G., Dhulipala, V.: Smart parking systems and sensors: A survey. In: 2012 International Conference on Computing, Communication and Applications (ICCCA). pp. 1–5 (2012)
- [21] Sappidi, R., Girard, A., Rosenberg, C.: Maximum achievable throughput in a wireless sensor network using in-network computation for statistical functions. *IEEE/ACM Transactions on Networking* 21(5), 1581–1594 (2013)
- [22] Schrank, D., Eisele, B., , T., L.: Urban Mobility Report 2012. Texas Transportation Institute, The Texas A& M University System, Texas USA (2012)
- [23] SFMTA: Sfpark: Putting theory into practice (August 2011), sfpark.org/wp-content/uploads/2011/09/sfpark_aug2011projsummary_print-2.pdf
- [24] Stanislawski, D., Vilajosana, X., Wang, Q., Watteyne, T., Pister, K.: Adaptive synchronization in ieee802.15.4e networks. *IEEE Transactions on Industrial Informatics* PP(99), 1–1 (2013)

-
- [25] Wang, Q.: Traffic analysis & modeling in wireless sensor networks and their applications on network optimization and anomaly detection. *Network Protocols and Algorithms* 2(1), 74–92 (2010)
- [26] Watteyne, T., Pister, K.: Smarter cities through standards-based wireless sensor networks. *IBM Journal of Research and Development* 55(1.2), 7:1–7:10 (2011)
- [27] Wsnet simulator for large scale wireless sensor networks, wsnet.gforge.inria.fr
- [28] Yan, G., Yang, W., Rawat, D., Olariu, S.: Smartparking: A secure and intelligent parking system. *IEEE Intelligent Transportation Systems Magazine* 3(1), 18–30 (2011)
- [29] Ye, W., Silva, F., Heidemann, J.: Ultra-low duty cycle mac with scheduled channel polling. In: *Proceedings of the 4th International Conference on Embedded Networked Sensor Systems*. pp. 321–334. *SenSys '06*, ACM, New York, NY, USA (2006), <http://doi.acm.org/10.1145/1182807.1182839>
- [30] Zing Zheng, W.R.: An adaptive control algorithm for traffic-actuated signals. *Transportation Research Part C: Emerging Technologies* 30 (May 2013)



**RESEARCH CENTRE
GRENOBLE – RHÔNE-ALPES**

Inovallée
655 avenue de l'Europe Montbonnot
38334 Saint Ismier Cedex

Publisher
Inria
Domaine de Voluceau - Rocquencourt
BP 105 - 78153 Le Chesnay Cedex
inria.fr

ISSN 0249-6399